NASA TECHNICAL NOTE

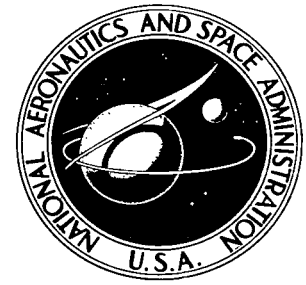

THE SIMULATION OF IONOSPHERIC CONDITIONS FOR SPACE VEHICLES

by Nobie H. Stone and Wilhelm K. Rehmann

George C. Marshall Space Flight Center
Marshall Space Flight Center, Ala. 35812

NATIONAL AERONAUTICS AND SPACE ADMINISTRATION • WASHINGTON, D. C. • AUGUST 1970

1. Report No.	2. Government Accession No.	3. Recipient's Catalog No.
NASA TN D-5894		

4. Title and Subtitle
The Simulation of Ionospheric Conditions for Space Vehicles

5. Report Date
August 1970

6. Performing Organization Code

7. Author(s)
Nobie H. Stone and Wilhelm K. Rehmann*

8. Performing Organization Report No.

9. Performing Organization Name and Address
George C. Marshall Space Flight Center
Marshall Space Flight Center, Alabama 35812

10. Work Unit No.
M435

11. Contract or Grant No.

12. Sponsoring Agency Name and Address

13. Type of Report and Period Covered
Technical Note

14. Sponsoring Agency Code

15. Supplementary Notes
* NRC — NASA Resident Research Associate. Prepared by Space Sciences Laboratory, Science and Engineering Directorate

16. Abstract

A plasma wind tunnel, designed for the simulation of ionospheric and solar wind conditions in an ultraclean environment using proper ion mass and energy and electron temperature, is described along with the system of diagnostic probes used for analysis. The operational characteristics of the system and the parameters of the drifting plasma indicate that the facility provides experimental capabilities in the areas of wake structure, sheath buildup, surface potential, drag forces, plasma-wave propagation, solar wind-magnetosphere interactions, and calibration of flight experiments.

EDITOR'S NOTE

17. Key Words (Suggested by Author(s))

18. Distribution Statement
Distribution Categories 11, 13, 25

19. Security Classif. (of this report)	20. Security Classif. (of this page)	21. No. of Pages	22. Price*
Unclassified	Unclassified	32	$3.00

*For sale by the Clearinghouse for Federal Scientific and Technical Information
Springfield, Virginia 22151

TABLE OF CONTENTS

LIST OF ILLUSTRATIONS

TECHNICAL NOTE D-

THE SIMULATION OF IONOSPHERIC CONDITIONS FOR SPACE VEHICLES

SUMMARY

A plasma wind tunnel facility capable of simulating ionospheric and solar-wind conditions in an ultraclean environment has been designed and fabricated. The correct ion mass and energy and electron temperature can be achieved, thereby decreasing the number of plasma parameters that must be scaled when conducting experiments. A Kaufman-type ion thruster, which has been modified to use various gases, is the plasma source. The ions exhausted from the thruster can be accelerated through a potential of 0 to 7 kV.

The diagnostic techniques used to analyze the system parameters include a Faraday cup, Langmuir and emissive probes, and an electrostatic energy analyzer that can be used for ions or neutrals.

The characteristics of the drifting plasma stream show the facility to be well suited to applied research on the space vehicle-ionospheric interaction, solar-wind phenomena, and the development of plasma probing techniques.

INTRODUCTION

During recent years, considerable interest has been exhibited in research on collisionless, drifting plasmas, which, in its application to space physics, provides valuable information on the interaction of space vehicles and the ionospheric plasma as well as solar-wind phenomena. In addition to the numerous theoretical publications in this field, some experimental work has been done by simulating certain environmental conditions of the ionosphere or the interplanetary plasma in earth-bound laboratories [1, 2, 3].

The plasma facilities of the Space Sciences Laboratory were set up and became operational during the past year. Research is planned in the area of space plasma simulation — more particularly, the simulation of ionospheric and solar-wind conditions in an ultra-clean environment using the proper ion mass and energy and electron temperature. This reduces to a minimum the number of plasma parameters to be scaled.

For this purpose, a plasma wind tunnel, consisting essentially of a Kaufman ion thruster and vacuum chamber, was assembled and calibrated. The ultrahigh vacuum chamber is cylindrical, measuring 1.2 m (4 ft) in diameter by 2.4 m (8 ft) in overall length, and provides a 1.07- by 1.8-m (3 1/2- by 6-ft) working space for experiments. The 15-cm diameter Kaufman ion thruster is mounted in a small bell-jar appendix in one end of the chamber and produces a high-velocity plasma beam along the axis of the chamber. The Kaufman engine is well suited for this application since it affords a wide range of control over the various plasma parameters.

Diagnostics are provided by a number of probes mounted on a traveling device that permits movement in two dimensions within the chamber (Fig. 1).

A second facility, consisting of an 45.7- by 76.2-cm (18- by 30-in.) bell-jar vacuum system and a discharge source, is being used to calibrate diagnostic equipment and conduct preliminary experiments in a quiescent plasma.

In addition to the aforementioned experimental capabilities, which include the problems of wake structure, sheath buildup, surface potential, drag forces, plasma-wave propagation, and solar-wind magnetosphere interactions, these facilities provide the opportunity for preparation and calibration of flight experiments.

VACUUM SYSTEM

The ultrahigh vacuum chamber is a horizontally mounted, cylindrical tank 1.2 m in diameter with an overall length of 2.4 m. A clear working space 1.07 m in diameter and 1.8 m long is available for conducting experiments. Access to the chamber is provided by a 1.2-m door at the front and a 45.7-cm port on the rear of the chamber. Numerous ports located along the top and sides of the chamber provide access feed-throughs for the various

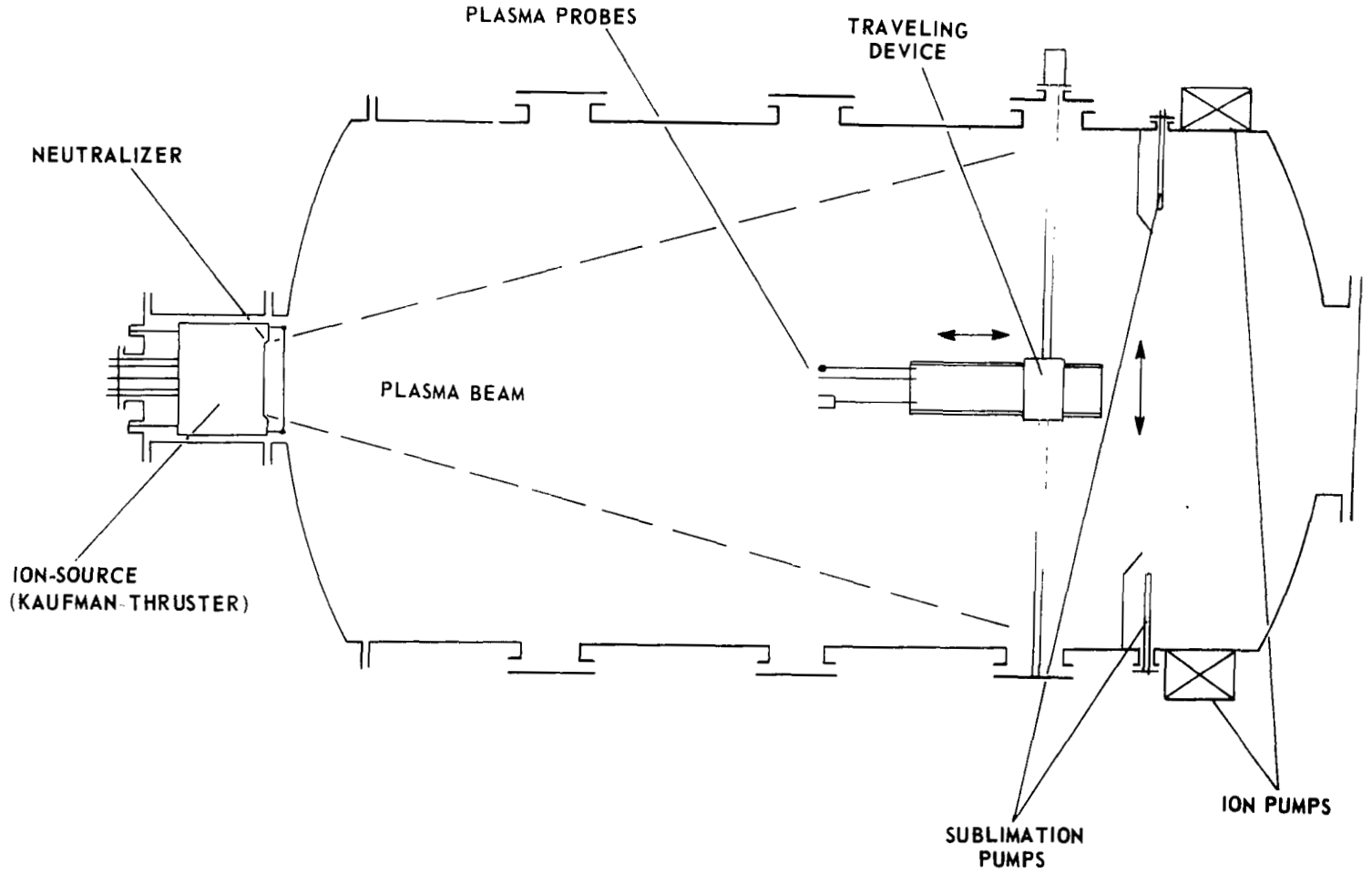

Figure 1. Schematic of the plasma wind tunnel.

experimental and diagnostic apparatus. In addition, a 30.5-cm port on the front end of the chamber allows mounting of the Kaufman ion thruster or other plasma sources.

Initial rough pumping of the chamber to 1 micron is accomplished using a 70.8-liter/sec mechanical blower, which is backed by a 9.9-liter/sec mechanical roughing pump. Back-streaming is prevented by a liquid nitrogen trap located between the blower and the chamber.

The ultrahigh vacuum pumping system consists of differential sputter ion pumps used in conjunction with a titanium sublimation pump and an LN_2 shroud. The ion pumps are rated at 1200 liters/sec and are mounted radially in the rear of the chamber such that they form an integral part of the chamber wall. Titanium is sublimated onto the rear wall of the chamber, providing a 26 000-liter/sec pumping capacity for nitrogen. The LN_2 shroud is an open-ended cylinder, 1.07 m in diameter and 1.8 m long, which encircles the working space in the chamber. With the chamber clean, dry, and empty, this system is capable of reaching 1×10^{-8} torr in 2 hr, maintaining a pressure of 1×10^{-6} torr while pumping against a calibrated nitrogen leak of 4×10^{-3} torr liter/sec, and reaching an ultimate pressure of 2×10^{-11} torr (as measured by an NRC Redhead gauge).

PLASMA SOURCE

The plasma beam is generated by a Kaufman-type, electron bombardment thruster with a beam diameter of 15 cm. This thruster was developed and manufactured by the NASA Lewis Research Center in Cleveland, Ohio and was desinged for the production of a 3-keV, 250-mA Hg^+-ion beam. To meet the technical requirements of the plasma wind tunnel, it was modified to produce a plasma beam of variable ion composition, energy and flux density (Fig. 2). In the simulation of ionospheric conditions, N_2^+ ions are accelerated through a potential of 9.35 V to achieve an orbital velocity of 8 km/sec; however, the solar wind can be simulated by using hydrogen ions and an acceleration potential of up to 7 kV.

During operation of the modified engine, a constant stream of neutral gas is fed by an automatically controlled leak into the front of the cylindrical discharge section of the engine. This automatic leak maintains a constant background pressure in the system. The gas molecules are ionized in the

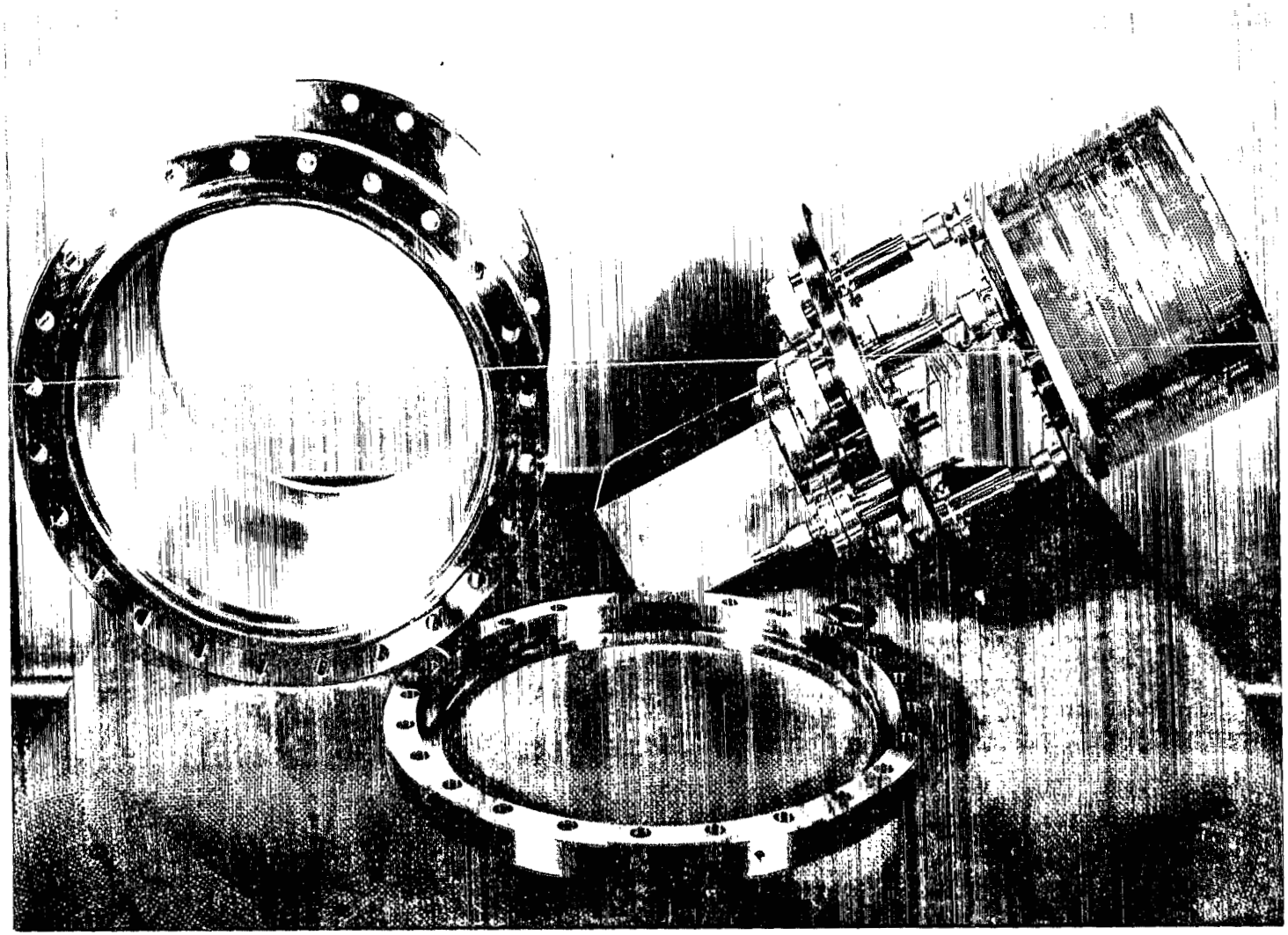

Figure 2. Modified Kaufman thruster.

discharge section by electron impact, the electrons being emitted from a tungsten ribbon cathode in the center of the engine and accelerated toward the outer cylindrical electrode by a steady potential, thus causing a nonself-sustaining plasma discharge. A magnetic field parallel to the axis of the engine provides higher ionization efficiency by producing spiral electron paths.

The ions are extracted from the discharge plasma by a voltage between the screen and acceleration grids which are located at the rear of the discharge section. The entire engine is biased on a positive potential that accelerates the ions extracted from the discharge. However, the kinetic energy of the ions in the plasma beam is also affected by the discharge voltage. The plasma potential in most of the discharge region of the engine is close to the anode potential so that a positive potential exist between the discharge plasma and the screen grid and contributes to the net ion acceleration.

An electron current, emitted from a hot tungsten wire in the exhaust of the engine, is injected into the extracted and accelerated ion beam, thus forming an electrically neutral, drifting plasma. Since the engine is biased on the positive acceleration potential of the plasma beam while the neutralizer is held at a slightly negative value, the plasma beam potential remains close to ground. A schematic of the engine is given in Figure 3.

The orientation of the engine within the bell-jar appendix of the vacuum system is adjustable in two dimensions so that proper alignment of the plasma beam with respect to the chamber axis can be attained. Because of the relatively small atomic mass of the gases to be used for ionospheric and solar wind simulation (nitrogen or hydrogen), both the thickness and hole diameters of the perforated screen plate had to be decreased to 0.508 mm. This modification provides for the attainment of reasonable extraction currents and matches the throughput of the engine to the pumping speed of the vacuum system so that the proper pressure for efficient ionization can be maintained within the discharge section of the engine while pressure in the experiment chamber remains low enough to ensure the existence of a collisionless medium. Typical operational parameters for the modified Kaufman ion thruster are given in Table 1.

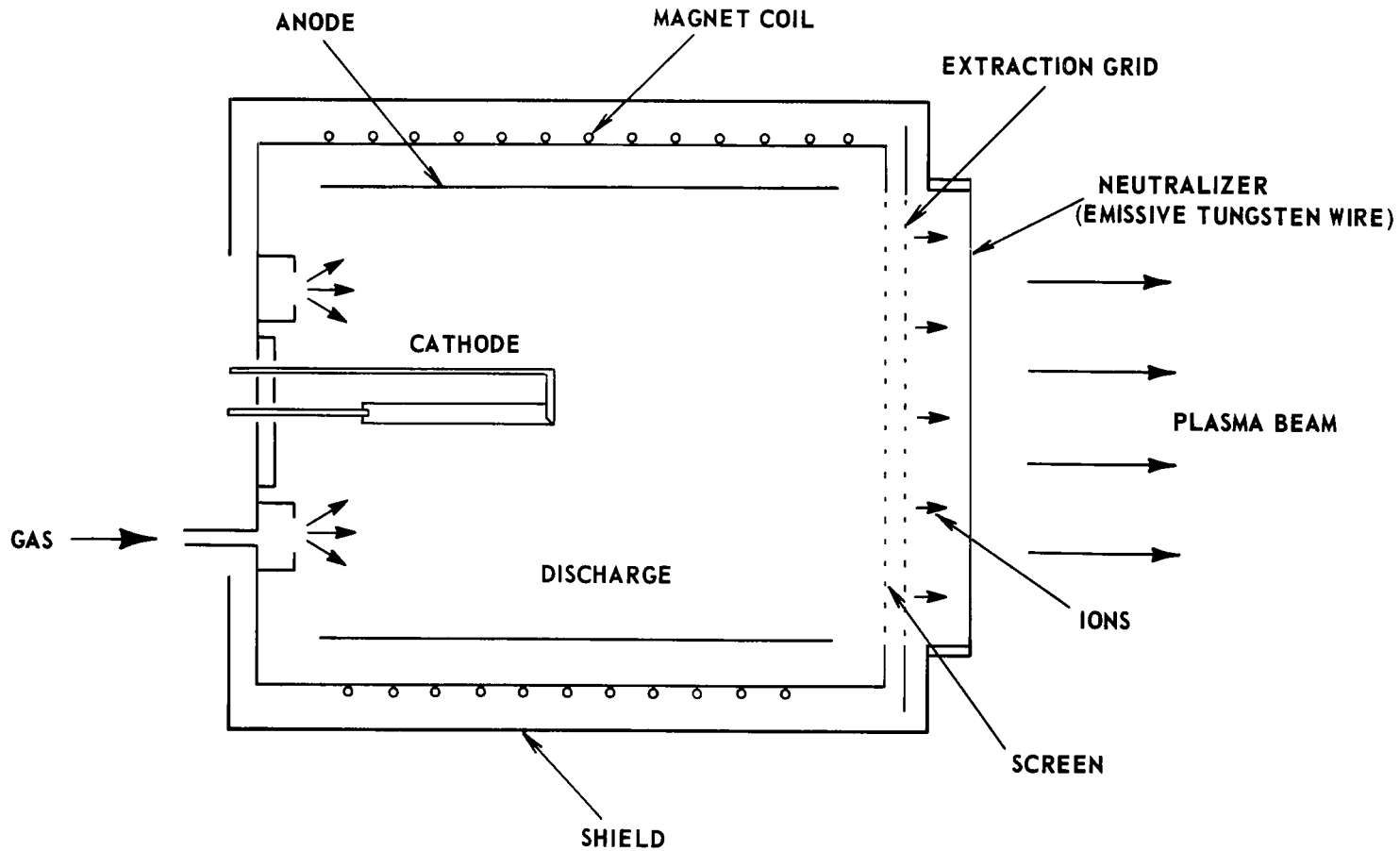

Figure 3. Schematic of the Kaufman thruster.

TABLE 1. TYPICAL OPERATIONAL PARAMETERS FOR THE KAUFMAN ION THRUSTER

Parameter	Symbol	Value
Background pressure	P_b	5×10^{-6} torr
Cathode current	I_c	60 A
Discharge voltage	U_d	50 V
Discharge current	I_d	0.25 A
Extraction voltage	U_e	100 V
Magnet current	I_m	6-9 A
Acceleration voltage	U_a	10 V
Beam current	I_b	10 mA

DIAGNOSTIC SYSTEM

The diagnostic equipment of the plasma wind tunnel includes a Langmuir probe, an emissive probe, a Faraday cup, and a 127-degree electrostatic energy analyzer with an adapter for the determination of the neutral particle energy spectrum. All of these plasma probes can be mounted on a traveling mechanism that moves horizontally across the full diameter and 27.9 cm parallel to the axis of the chamber.

Langmuir Probe

The Langmuir probe is essentially a small metallic electrode, immersed into the plasma. Under certain conditions, the local magnitudes of the electron temperature, the ion density, and the potential of the undisturbed plasma can be derived from the current-voltage characteristic of the probe [4]. However, in spite of the mechanical simplicity, the theory of the Langmuir probe is rather complicated and sets numerous restrictions on the interpretation of the data.

The Langmuir probe characteristic curve consists of three distinct parts, each of which is associated with a certain mode of operation. At large negative potentials of the probe with respect to the plasma potential, the current is almost completely composed of positive ions. The contribution of this ion saturation current to the total probe current at more positive potentials is small and can often be neglected; however, compensation can be made, when necessary, by extrapolation into higher potential regions.

As the probe potential becomes less negative, electrons begin to reach the probe because of their thermal energy. This is designated as the electron retarding region of the characteristic curve. For a Maxwellian energy distribution, we obtain an exponential current-voltage relationship

$$I = I_0 \exp\left(\frac{e\Delta U}{kT_e}\right) \quad , \tag{1}$$

where ΔU is the potential difference between probe and plasma (i.e., $\Delta U = U_p - U$), I_0 = probe current for $\Delta U = 0$, and T_e = electron temperature. From this part of the characteristic curve the electron temperature can be derived.

The third region of the probe current-voltage curve is characterized by an electron saturation current and occurs for positive values of ΔU. This part of the curve varies significantly with the geometrical configuration of the probe. In a first-order approximation for cylindrical probes, this characteristic can be described by

$$I = I_0 \left(1 + \frac{e\Delta U}{kT_e}\right)^{\frac{1}{2}} \quad . \tag{2}$$

The intersection point of the extrapolated curves for the electron retarding and saturation regions yields the plasma potential, U_0, and the saturation current, I_0. Using T_e from equation (2), the plasma density can be obtained from the expression,

$$N_0 = \frac{I_0}{A_e}\sqrt{\frac{2\pi m}{kT_e}} \quad ,$$

where A_e is the probe cross sectional area.

The Langmuir probe used in the plasma wind tunnel is a flat disc 2.54 cm in diameter. Figure 4 shows a typical Langmuir characteristic.

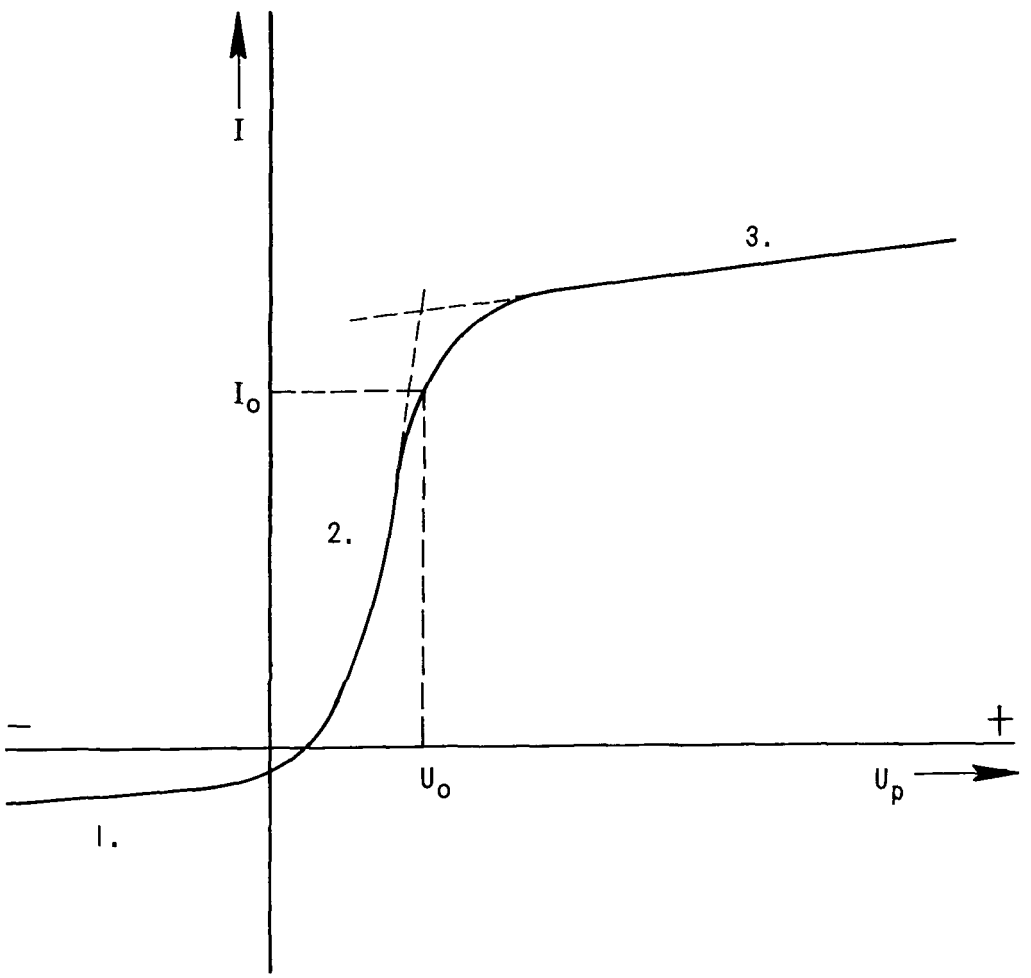

Figure 4. A typical Langmuir probe curve.

For a fast reduction of the Langmuir probe data, an instrument was built that compensates for ion current and gives a direct readout of information on the electron temperature, thus permitting the coarse determination of the electron current saturation point [5].

Emissive Probe

In addition to the Langmuir probe, an emissive probe, which is essentially a hot, emissive tungsten wire immersed into the plasma, is used to determine the plasma potential. By measuring the total probe current at an emissive condition for various probe potentials and subtracting the usually small Langmuir current, which is determined at a nonemissive condition, the current-voltage characteristic of the emitted electron current can be obtained. This curve is similar to a Langmuir probe characteristic except that the potential is inverted; the inversion results from the emitted current flowing in the opposite direction to that of the Langmuir current. The intersection of the emission-limited region of the curve with the Boltzmann region occurs at the plasma potential. The emissive probe is superior to the Langmuir probe in that a higher probe current is provided which permits a more precise determination of the plasma potential.

The emissive probe used in this diagnostic system is a tungsten wire loop 0.05-mm (0.002-in.) diameter, which protrudes 0.64 cm (0.25 in.) from its shielding. It should be noted that the wire must be unipotential during measurements; thus, the heating current must be intermittently pulsed off for taking data. This is accomplished by an electronic circuit that also reduces the data from the characteristic signal automatically to provide a direct instrument reading of the plasma potential. The error of the potential determination is in the range of approximately $\pm$ 0.01 V [6].

Faraday Cup

The current density of the plasma beam is measured by a Faraday cup, which is a relatively simple device used for charged particle collection. In principle, the device consists of a shielding container, which is held at the plasma potential to minimize any perturbation of the plasma, and has a small aperture through which charged particles enter and impinge on an internal conducting cup that serves as a charge collector. This cup is, in turn, connected through a shielded lead to an electrometer, which monitors the magnitude of the current.

The current collected by the Faraday cup is related to other parameters of the plasma beam through the expression $nZevA$, where n = ion number density, Ze = ionic charge, v = ion beam velocity, and A = aperture area of the Faraday cup. Thus, in addition to the beam current density, the Faraday cup can also provide an imput to the equations through which other parameters are determined.

Unfortunately, this rather simple picture of the Faraday cup is clouded by low-sensitivity, secondary electron emission, charge accumulation on insulating materials, and the fact that charges of either sign can enter the aperture. However, these problems can be solved by proper design and choice of electronic readout equipment. Charges of the desired polarity can be selected by placing a biased grid over the aperture. Sensitivity could be increased by enlarging the aperture, but this would result in an increased production of secondary electrons. Therefore, attainment of a useful operating range for the device requires a sensitive electrometer for readout. Secondary electron emission can then be minimized by constructing a deep collector cup so that the solid angle of the entrance, viewed from the bottom, is $<<2\pi$ and by designing the shielding container and grids so that the charged particles entering the cup are well collimated [7].

Energy Analyzer

The particle energy of a plasma beam can be analyzed by means of a variable retarding potential that gives the integral of the energy spectrum, or by particle deflection by electric or magnetic fields; the latter method usually provides better accuracy by measuring the direct spectrum. Since stray magnetic fields would cause perturbations of the plasma flow, an electrostatic field was used to produce a 127-degree deflection in a cylindrical electrode geometry; this deflection angle (more exactly $\frac{\pi}{\sqrt{2}}$) provides, in a first-order approximation, an angular focusing of particles of a distinct energy on the exit slot for small incident angles with respect to the axis (Fig. 5).

The radius of the axis for the deflection section, r_0, is 50 mm, and the electrode separation is 15 mm, resulting in a ratio of the deflection voltage to particle energy of

$$\frac{U_{defl}}{E} = \frac{2}{e} \ln\left(\frac{R_1}{R_2}\right) = \frac{0.6}{e} \quad .$$

This ratio was chosen particularly for the determination of particle energies ranging to one hundred eV, which are characteristic for ionospheric plasma simulation. The electrode separation limits the maximum and minimum radii of the off-axis particle trajectories, and, hence, it follows by the equation

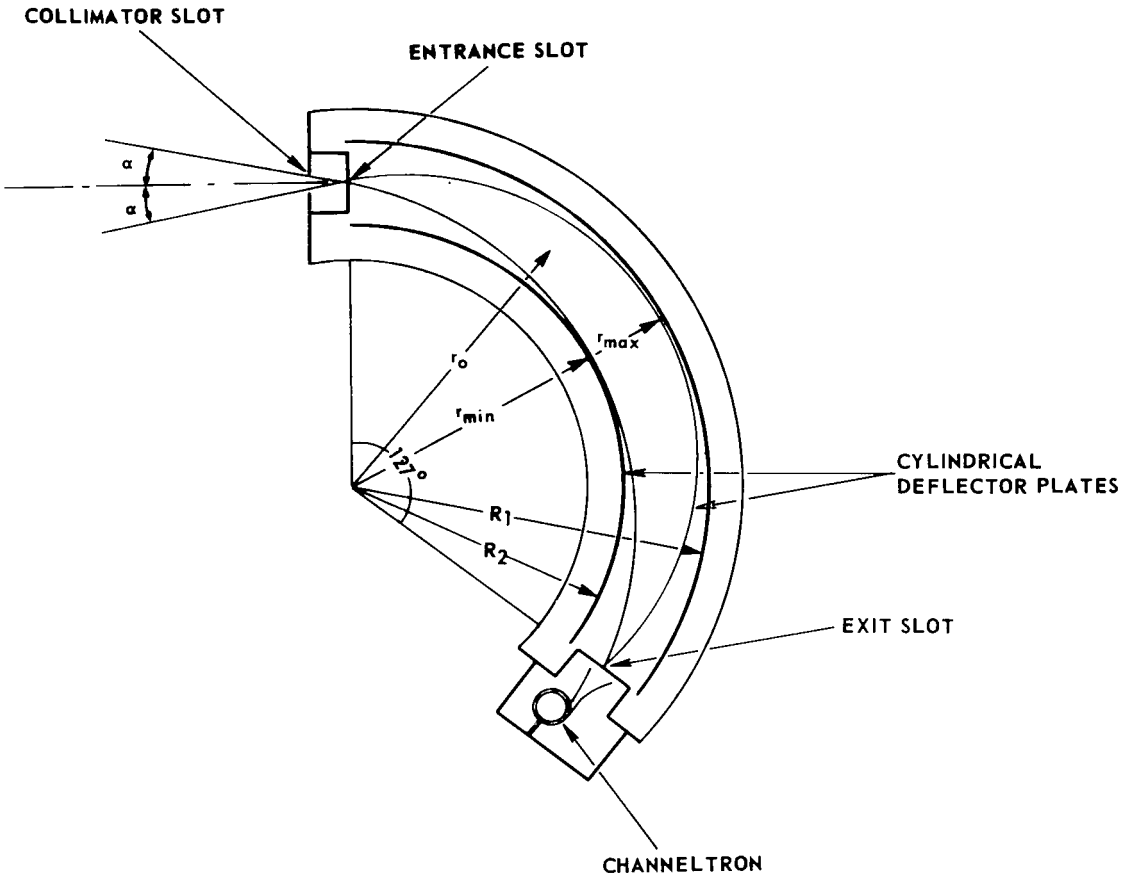

Figure 5. Schematic of the electrostatic energy analyzer.

$$r_{max,min} = r_0\left(1 \pm \frac{\alpha_m}{\sqrt{2}}\right)$$

that the maximum vertical half angle, α_m, of the incident particles to be focused on the exit is slot limited to 11.5 degrees. A collimator window in front of the entrance slot eliminates particles with a larger incident angle. The corresponding maximum lateral half angle amounts to 4 degrees.

The maximum image width, B, for particles incident over the full aperture angle would be 2.7 mm, according to the relation $B = \frac{4}{3}\alpha^2 r_0$;

however, an exit slot of 2 mm was chosen to improve resolution. The velocity dispersion D_v of the deflection defined by $D_v = dx \frac{v}{dv}$ [1], is given for cylindrical electrostatic fields by $D_v = 2r_0$. The deflection radius and the exit slot width of this analyzer implies a velocity resolution of $\frac{v}{dv} = 50$. The particles passing the exit slot are detected by either a Faraday cup or, for less dense plasma beams, a Channeltron particle detector which provides increased sensitivity. It should be noted that all formulas given here are valid only for nonrelativistic particles [8].

The adapter for determining the energy spectrum of the neutral particle component of the plasma stream, mounted onto the front of the collimator window of the energy analyzer, operates as follows: The ions and electrons are reflected by a positively and a negatively biased grid in the front aperture. These biased grids are shielded from the plasma and the internal ionization section by two additional grids, which are maintained at the plasma potential. After passing the reflecting grids, the neutral particles are ionized by two electron beams that are emitted from negatively biased tungsten filaments and flow in opposite directions, perpendicularly to the neutral particle beam (Fig. 6).

The ionized neutrals then pass into the 127-degree energy analyzer where their energy is determined by the previously discussed method.

SYSTEM CHARACTERISTICS

Characteristics of the plasma wind tunnel, determined with the instruments described in the Diagnostic System Section are given in the following section and show the effect of various engine parameters and typical values of beam parameters.

Engine Parameters

The dependence of engine performance on the variation of different engine parameters is presented in Figures 7 through 10. In Figures 7 and 8

---

1. dx = image line deviation; dv = velocity deviation

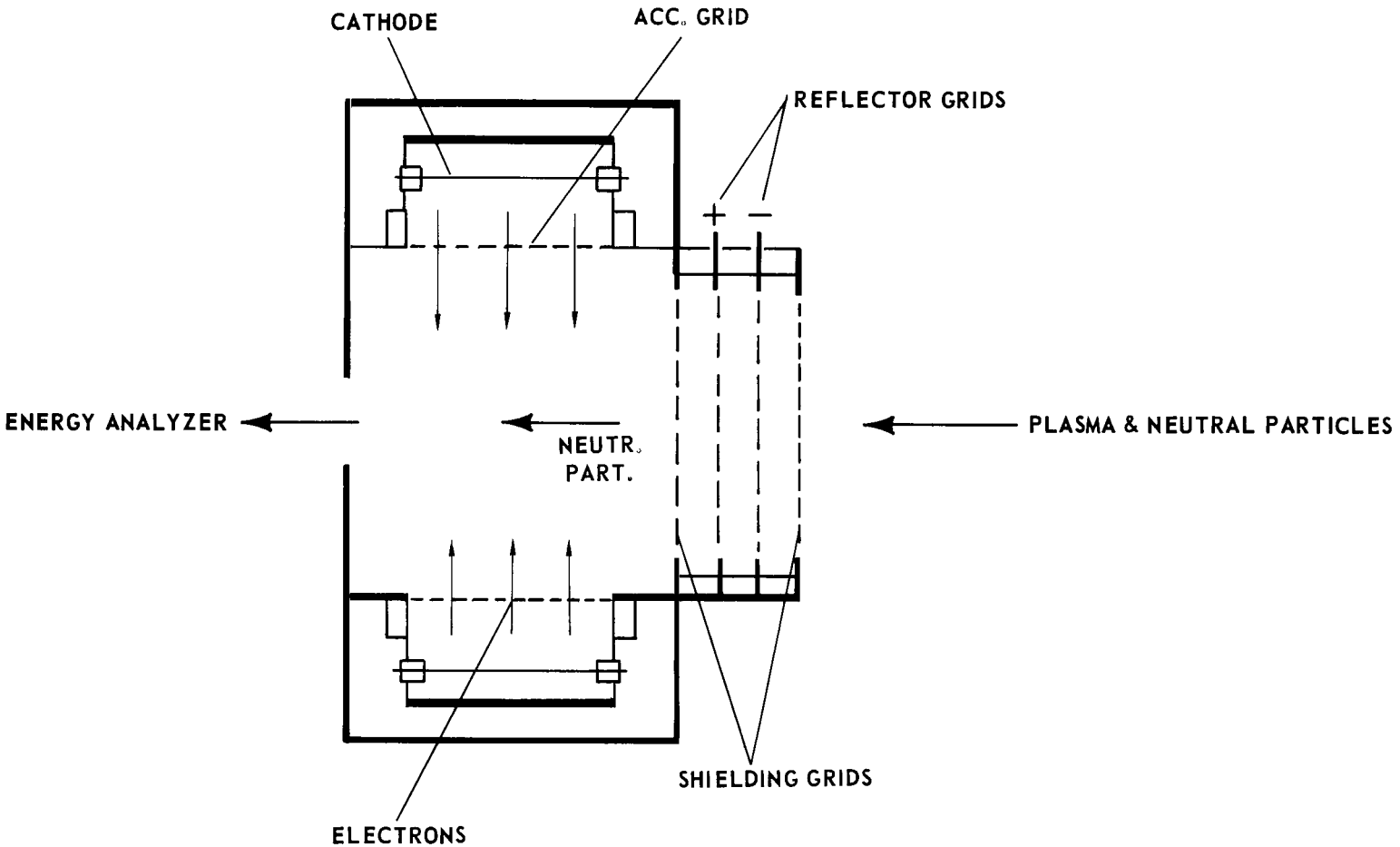

Figure 6. Schematic of the neutral particle adapter.

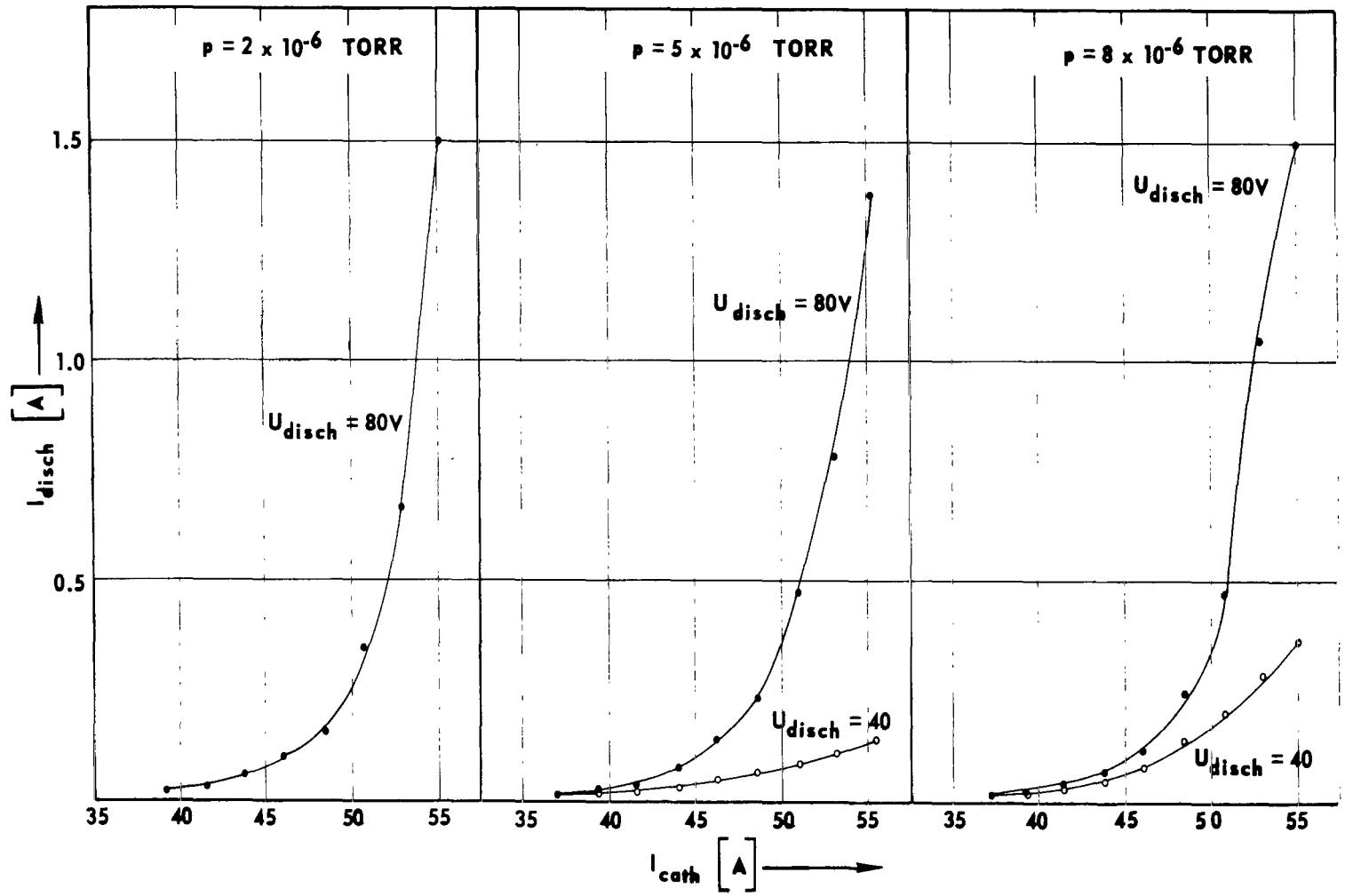

Figure 7. Dependence of discharge current on cathode current.

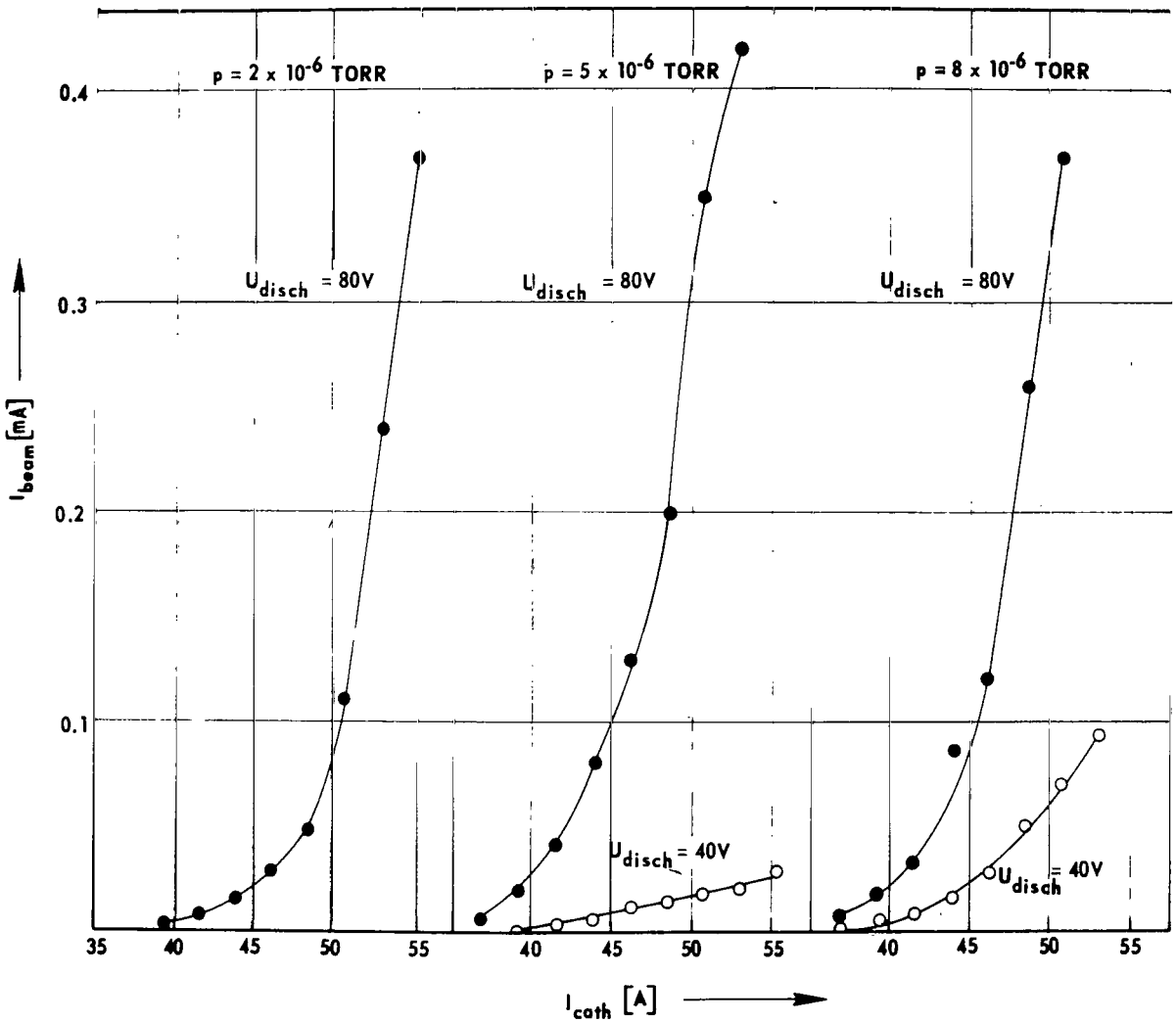

Figure 8. Dependence of engine beam current on cathode current.

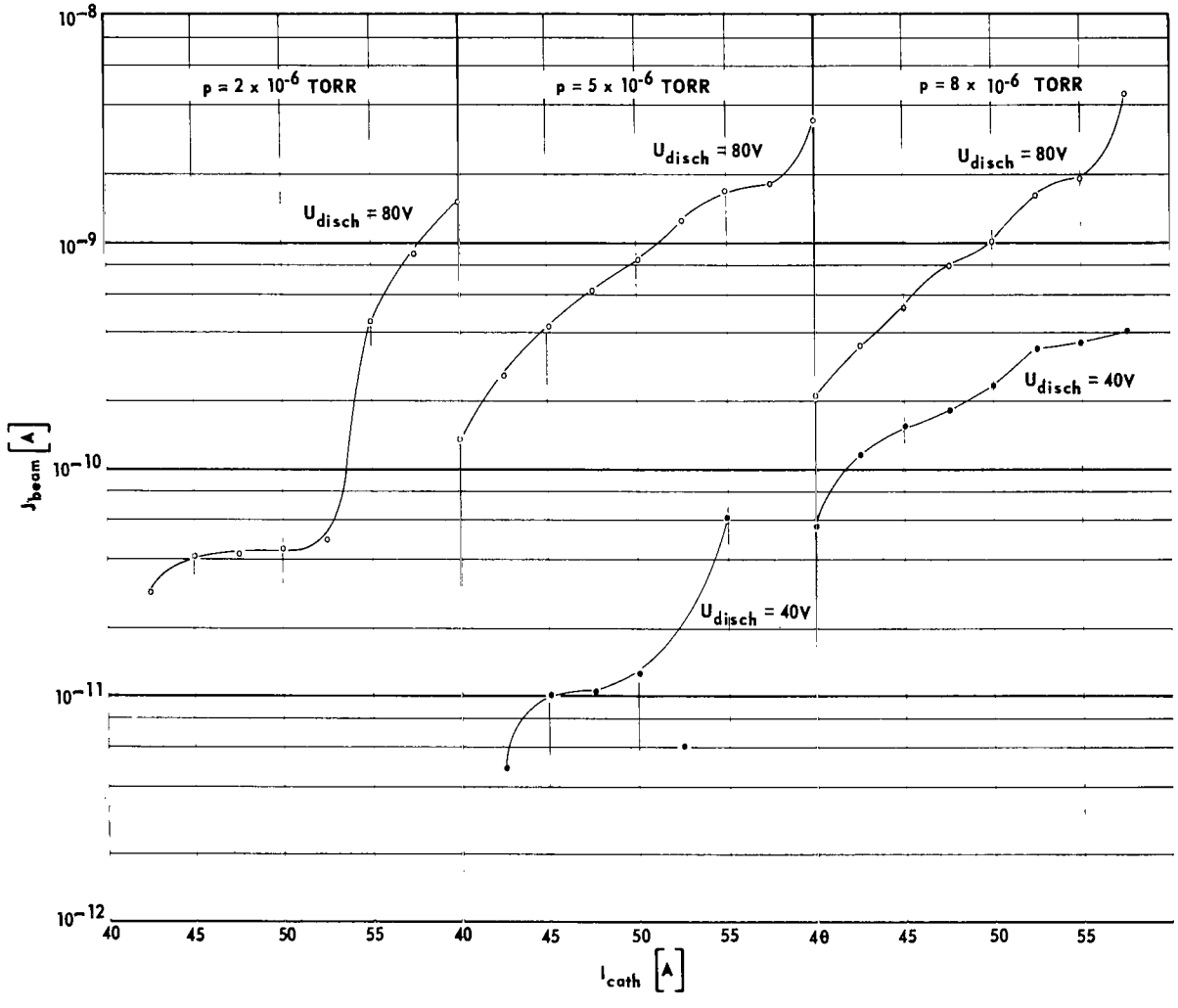

Figure 9. Dependence of unneutralized beam current density on cathode current.

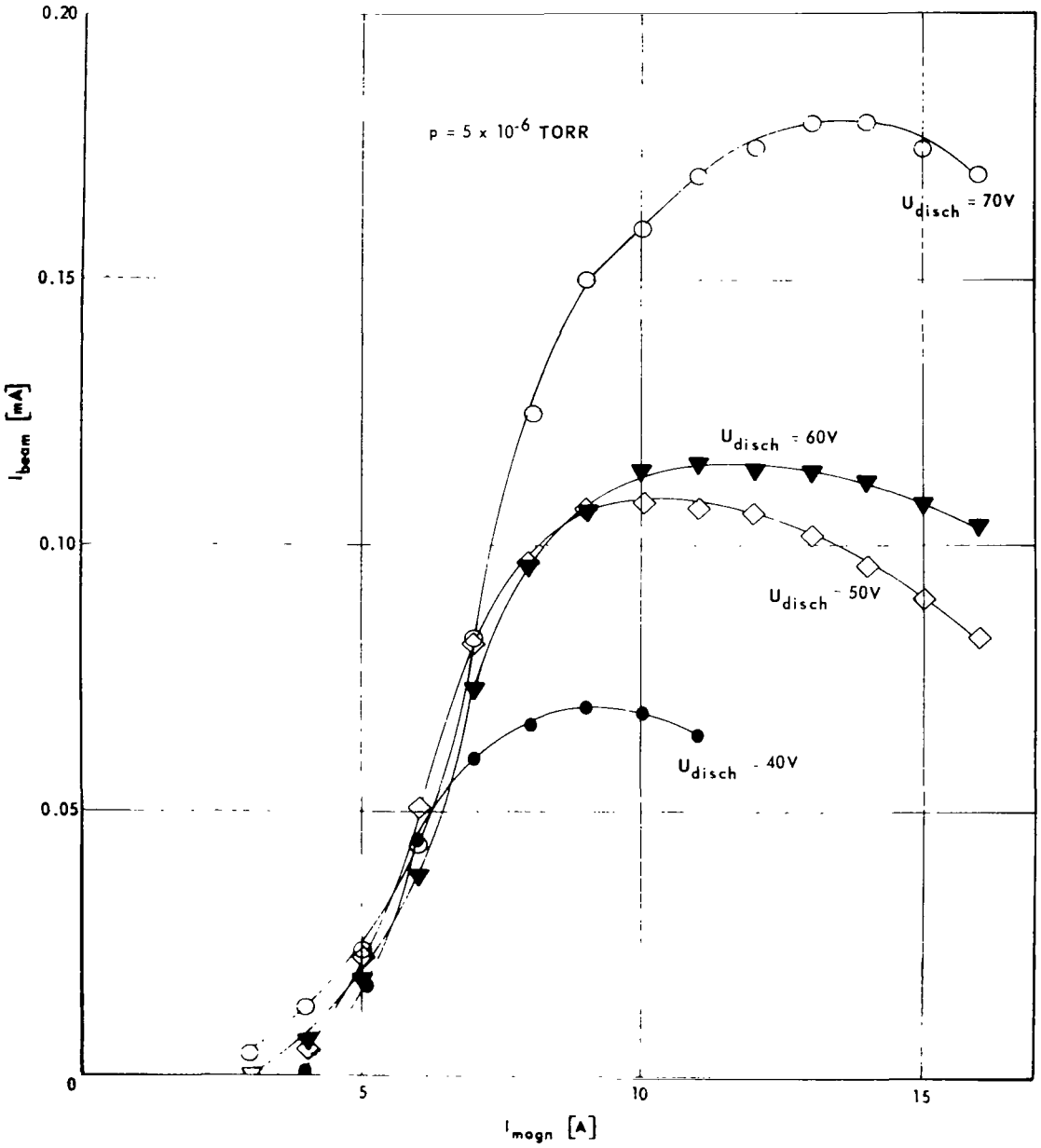

Figure 10. Dependence of engine beam current on magnet current.

the characteristics of the discharge and beam currents are plotted as functions of the cathode current for two different discharge potentials and three settings of the system pressure. (System pressure is directly proportional to the pressure in the discharge section of the engine.) The magnet current was held constant at a value that provided an optimum performance of the engine.

An increase in cathode current results in a nonlinear increase of the discharge and beam currents by enhanced thermionic emission of the cathode in accordance with the Richardson law, but also results in a shorter cathode lifetime caused by faster evaporation of the filament material. Likewise a variation of the discharge voltage from 40 to 80 V increases the discharge and beam currents by a factor of 3 to 6; however, the sputtering rate of the cathode grows by approximately two orders of magnitude. At high discharge voltages, the beam current characteristics are not substantially affected by variations of the system pressure while at lower voltages a pressure drop results in a considerable decrease in the beam current. At 40 V and 2×10^{-6} torr, the discharge could not be ignited.

To run the engine in a range of optimum conditions for obtaining maximum cathode lifetime and current output, the discharge voltage was usually set at 50 V, the pressure to 5×10^{-6} torr and the cathode current between 50 and 60 A, according to the desired beam current.

In Figure 9, the current density of the unneutralized ion beam is plotted as a function of the cathode current with discharge voltage and system pressure as parameters. These data were measured by means of a Faraday cup located in the beam about 1.4 m downstream from the engine. The current density characteristics deviate considerably in shape from the curves of the total beam current as a result of increased beam divergence produced by electrostatic repulsion which occurs in the unneutralized beam.

The dependence of the total beam current on the magnetic field in the discharge section of the engine (represented by the magnet current) is shown in Figure 10 for a constant cathode current of 50 A, a system pressure of 5×10^{-6} torr, and four different settings of the discharge voltage. All of these plots display maximum or plateau regions. Increased magnet current beyond the maximum results first in a decrease of the beam current and finally in oscillations in the discharge which becomes unstable.

Beam Parameters

The kinetic energy of the plasma ions is determined by the 127-degree electrostatic energy analyzer. The actual acceleration potential, deduced from this measurement, is considerably higher than the acceleration voltage, U_{acc}, of the engine, i.e., the potential difference between system ground and engine ground. This is caused by the potential difference between the discharge plasma and the screen, which produces an additional ion acceleration. Under normal working conditions 90 to 95 percent of the anode-cathode potential drop occurs near the cathode (cathode fall) and so the major part of the discharge plasma is only a few volts below anode potential, which is typically 40 to 80 V. Figure 11 shows the relation between ion energy, E_{ion}, and acceleration potential, U_{acc}, for different discharge voltages.

The electron temperature of the neutralized plasma beam is determined by a Langmuir probe (shielded disk type). The Langmuir characteristic, recorded with the neutralizer biased on ground potential, is shown in Figure 12. The graphic analysis yields an electron temperature of 4000° K; for ionospheric simulation, this would correspond to an altitude of 3000 km.

The current density profile of the neutralized beam, measured by the Faraday cup located 1.4 m downstream from the engine, is plotted in Figure 13 for an ion energy of 48 eV. The dotted part of the profile had to be extrapolated because of a disturbance of the beam in this region, caused by two wave transmission electrodes mounted upstream. It was not convenient to remove these probes from the chamber at the time of the test; however, they could be moved about in the beam, which resulted in a corresponding movement of the disturbed region of the profile. If the two points where the current density amounts to 90 percent of its maximum value are considered the geometrical limits of the beam, the divergence angle is found to be 1 3/4 degrees. This provides a region which is 23.5 cm in diameter and has uniform beam current density (10-percent variation) for conducting experiments. For 88.5-eV beam energy, the divergence angle decreases to 3/4-degree half angle, or a workable beam area 19.5 cm in diameter. Hence, for more energetic beams the working area would be smaller.

The plasma wind tunnel facility has, to date, been utilized for the experimental study of ion acoustic wave propagation in the simulated environment of a satellite traveling through the ionospheric plasma. In addition to continued

use in ionospheric experiments, further modifications to the Kaufman thrustor plasma source are planned so that certain aspects of the solar wind can be simulated.

George C. Marshall Space Flight Center
National Aeronautics and Space Administration
Marshall Space Flight Center, Alabama 35812, April 27, 1970
124-09-00-00-62

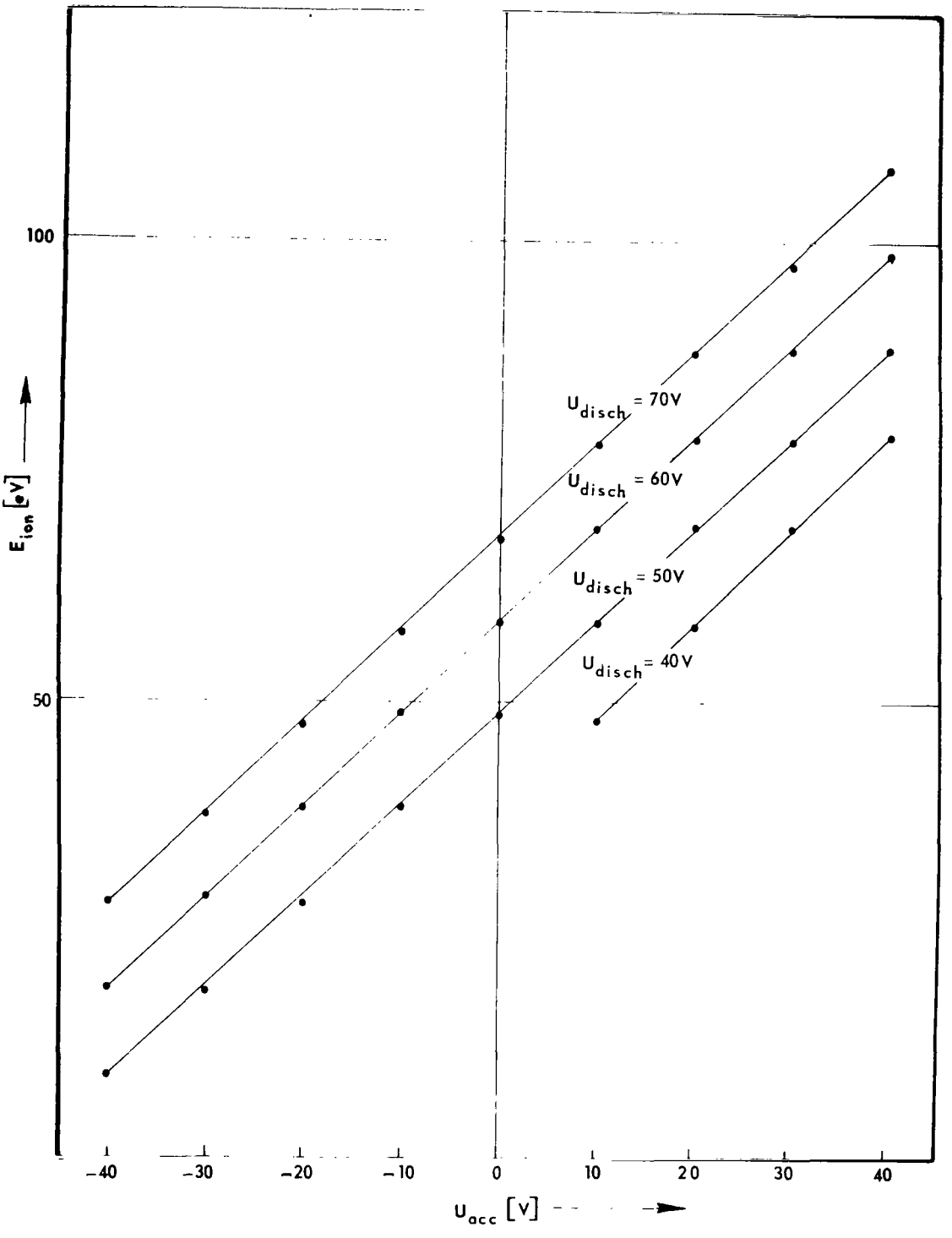

Figure 11. Ion kinetic energy versus acceleration potential.

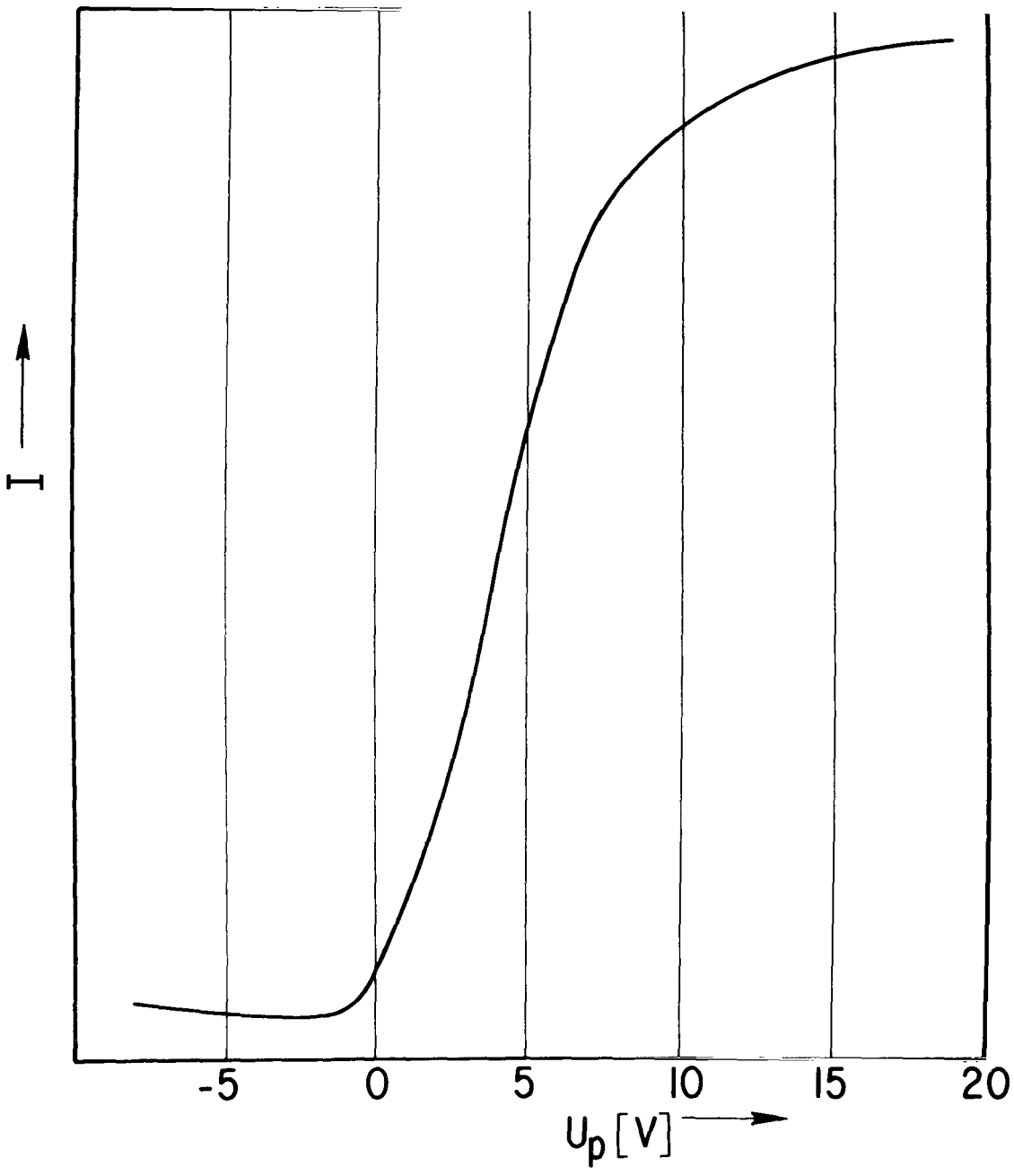

Figure 12. Langmuir characteristic produced by beam .

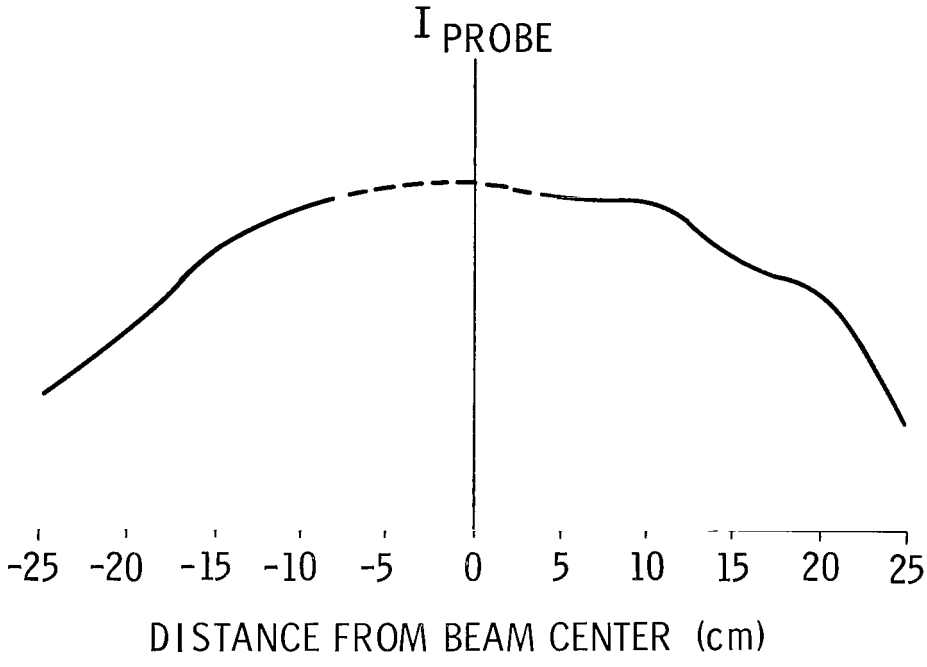

Figure 13. Beam current density profile.

REFERENCES

1. Hall, D. F.; Kemp, R. F.; and Sellen, J. M., Jr.: Generation and Characteristics of Plasma Wind-Tunnel Streams. AIAA Journal, vol. 3, no. 8, August 1965, pp. 1490-1497.

2. Sellen, J. M., Jr.; Investigation of Ion Beam Diagnostics. TRW, NASA Contract NAS8-1560, April 1964.

3. Sellen, J. M., Jr.; Bernstein, W.; and Kemp, R. F.: Generation and Diagnosis of Synthesized Plasma Streams. The Review of Scientific Instruments, vol. 36, no. 3, March 1965, pp. 316-322.

4. Chen, Francis F.: Electric Probes. Plasma Diagnostic Techniques, R. H. Huddelstone and S. L. Leonard, ed., Academic Press (New York), 1965, pp. 113-200.

5. Crawford, F. W.; and Hays, R. S.: Circuit for the Rapid Determination of Langmuir Probe Data. The Review of Scientific Instruments, vol. 33, no. 12, December 1962, pp. 1387-1391.

6. Kemp, R. F.; and Sellen, J. M., Jr.: Plasma Potential Measurements by Electron Emissive Probes. Review of Scientific Instruments, vol. 37, no. 4, April 1966, pp. 455-461.

7. Osher, J. E.: Particle Measurements. Plasma Diagnostic Techniques, R. H. Huddlestone and S. L. Leonard, ed., Academic Press (New York), 1965, pp. 537-540, 556.

8. Bainbridge, K. T.: Charged Particle Dynamics and Optics, Relative Isotopic Abundances of the Elements, Atomic Masses. Experimental Nuclear Physics: Vol. I, L. Segré, ed., John Wiley & Sons, Inc. (New York), 1960.

NASA-Langley, 1970 —— 11 M435

NATIONAL AERONAUTICS AND SPACE ADMINISTRATION
WASHINGTON, D. C. 20546
OFFICIAL BUSINESS

FIRST CLASS MAIL

POSTAGE AND FEES PAID
NATIONAL AERONAUTICS AND
SPACE ADMINISTRATION

02U 001 36 51 3DS 70195 00903
AIR FORCE WEAPONS LABORATORY /WLOL/
KIRTLAND AFB, NEW MEXICO 87117

ATT E. LOU BOWMAN, CHIEF, TECH. LIBRARY

POSTMASTER: *If Undeliverable (Section 158 Postal Manual) Do Not Return*

"The aeronautical and space activities of the United States shall be conducted so as to contribute . . . to the expansion of human knowledge of phenomena in the atmosphere and space. The Administration shall provide for the widest practicable and appropriate dissemination of information concerning its activities and the results thereof."

—NATIONAL AERONAUTICS AND SPACE ACT OF 1958

NASA SCIENTIFIC AND TECHNICAL PUBLICATIONS

TECHNICAL REPORTS: Scientific and technical information considered important, complete, and a lasting contribution to existing knowledge.

TECHNICAL NOTES: Information less broad in scope but nevertheless of importance as a contribution to existing knowledge.

TECHNICAL MEMORANDUMS: Information receiving limited distribution because of preliminary data, security classification, or other reasons.

CONTRACTOR REPORTS: Scientific and technical information generated under a NASA contract or grant and considered an important contribution to existing knowledge.

TECHNICAL TRANSLATIONS: Information published in a foreign language considered to merit NASA distribution in English.

SPECIAL PUBLICATIONS: Information derived from or of value to NASA activities. Publications include conference proceedings, monographs, data compilations, handbooks, sourcebooks, and special bibliographies.

TECHNOLOGY UTILIZATION PUBLICATIONS: Information on technology used by NASA that may be of particular interest in commercial and other non-aerospace applications. Publications include Tech Briefs, Technology Utilization Reports and Notes, and Technology Surveys.

Details on the availability of these publications may be obtained from:

SCIENTIFIC AND TECHNICAL INFORMATION DIVISION

NATIONAL AERONAUTICS AND SPACE ADMINISTRATION

Washington, D.C. 20546